



# Doppler shifts in the transition region and corona

## Mass cycle between the chromosphere and the corona

P. Zacharias<sup>1</sup>, S. Bingert<sup>1</sup>, and H. Peter<sup>2</sup>

<sup>1</sup> Kiepenheuer Institut für Sonnenphysik – Schöneckstrasse 6, D-79104 Freiburg, Germany  
e-mail: p.zacharias@kis.uni-freiburg.de

<sup>2</sup> Max-Planck-Institut für Sonnensystemforschung – Max-Planck-Strasse 2, D-37191  
Katlenburg-Lindau, Germany

**Abstract.** Emission lines in the transition region and corona show persistent line shifts. It is a major challenge to understand the dynamics in the upper atmosphere and thus these line shifts, which are a signature of the mass cycle between the chromosphere and the corona. We examine EUV emission line profiles synthesized from a 3D MHD coronal model of a solar-like corona, in particular of an active region surrounded by strong chromospheric network. This allows us to investigate the physical processes leading to the line Doppler shifts, since we have access to both, the synthetic spectra and the physical parameters, i.e. magnetic field, temperature and density in the simulation box. By analyzing the evolution of the flows along field lines together with the changing magnetic structure we can investigate the mass cycle. We find evidence that loops are loaded with mass during a reconnection process, leading to upflows. After the loops disconnect from the reconnection site, they cool and drain which leads to the observed redshifts. Previous 1D loop models (neglecting the 3D nature) assumed that heating leads to evaporation and upflows followed by a cooling phase after the heating stops. The scenario modeled here is quite different, as it shows that the continuously changing three-dimensional magnetic structure is of pivotal importance to understand the mass balance between the chromosphere and the corona.

**Key words.** Sun: corona – Sun: EUV Spectroscopy – Stars: corona

### 1. Introduction

Doppler shift observations of the quiet Sun disk center show redshifts in optically thin transition region EUV emission lines and blueshifts in coronal EUV emission lines (Peter & Judge 1999). Spectra synthesized from 3D MHD models of the solar corona

(Gudiksen & Nordlund 2002, Peter et al. 2004, 2006) show a good match with the observed Doppler shifts in the transition region lines (Fig. 1). However, so far, the models are not reproducing the observational blueshifts for the coronal lines.

We examine extreme-ultraviolet emission line profiles synthesized from a 3D MHD coronal model (Bingert et al. 2009, Zacharias et al.

---

*Send offprint requests to:* P. Zacharias

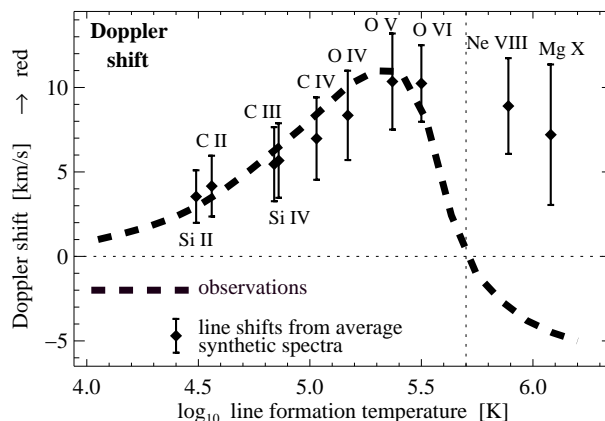


**Fig. 1.** Comparison of the observed Doppler shifts (thick dashed line, data from Peter & Judge 1999) with the predictions of our 3D MHD model. The diamonds show the average Doppler shifts computed from the synthesized emission line profiles for an arbitrarily chosen single timestep ( $t=30$  min) of the simulation. The height of the error bars corresponds to the standard deviation of the Doppler shifts at that timestep. The line shifts from the average spectra of our simulation are similar to the results of Peter et al. (2004, 2006).

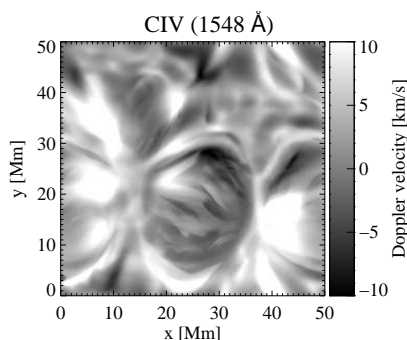


**Fig. 2.** Doppler shifts in the C IV (1548 Å) line at timestep  $t=30$  min of the simulation run when looking at the simulation box from straight above.

dient in the transition region. The full energy equation is solved, including heat conduction and radiative losses, which is essential for the spectral line synthesis that is carried out. The heating mechanism is due to the braiding of the magnetic field lines by the photospheric foot-point motions that can transfer the work directly into heat in the corona by dissipation of currents (Parker 1972, 1983). Since we have access to both, the synthetic spectra and the physical parameters, i.e. magnetic field, temperature and density in the simulation box, we can investigate the physical processes that lead to the emission line Doppler shifts.

## 2. Spectral line synthesis

2009) of a solar-like corona, in particular of an active region surrounded by strong chromospheric network. These models are similar to previous numerical experiments by Gudiksen & Nordlund (2005a, 2005b). Using the Pencil code (Brandenburg & Dobler 2002) the simulations are performed on a  $256^3$  grid for a box of the size  $50 \times 50 \times 30 \text{ Mm}^3$ . Periodic boundary conditions are applied in the horizontal directions. In the vertical direction a non-uniform mesh accounts for the strong temperature gra-

The emissivity of an optically thin emission line is a function of temperature and electron density only. It can therefore be directly calculated from the MHD simulation data according to  $\epsilon = h\nu A_{21} n_2$ , where  $h\nu$  is the energy,  $n_2$  is the number density of the upper level, and  $A_{21}$  is the Einstein coefficient of the transition from an upper level 2 to a lower level 1. For the calculations ionization equilibrium is assumed even though time-dependent ionization should be included. However, it was shown by Peter

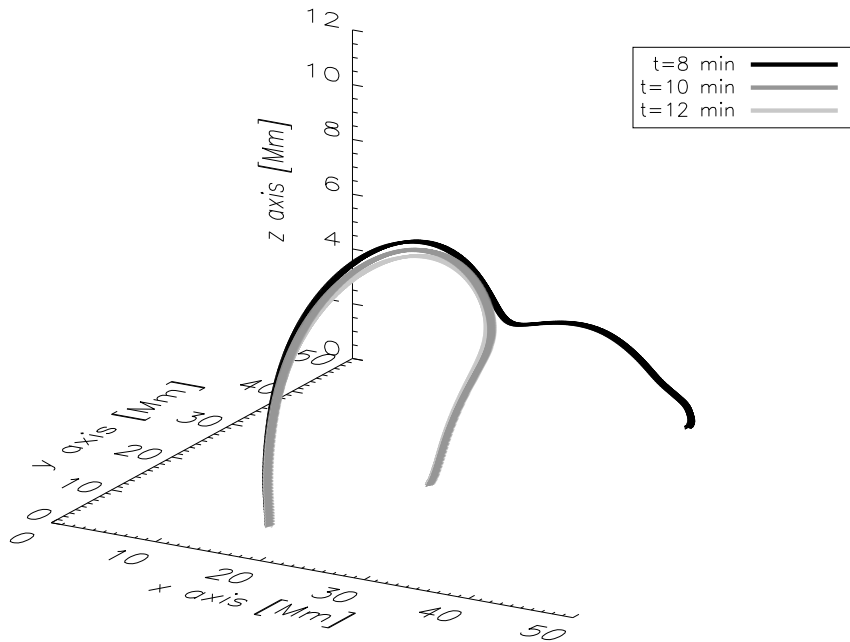


**Fig. 3.** Temporal evolution of field line near small X-type reconnection site for some five minutes of simulation time.

et al. (2006) that the ionization and recombination times in the coronal and transition region plasma are mostly smaller than the typical hydrodynamic timescale and thus, in a first approximation, the assumption of ionization equilibrium is not too bad. The line width is given by the thermal width  $\omega_{th} = \sqrt{2k_B T / m_{ion}}$  of the line. The line profiles are integrated along the line of sight to give maps of spectra that can be analyzed like real observations resulting in maps of line intensity, line shift, and line width. For a more detailed discussion on how these quantities are calculated, the reader is referred to Peter et al. (2006).

### 3. Origin of Doppler shifts

For the C IV line an average redshift of +6.7 km/s is obtained for the 30 minute simulation run. Fig. 1 shows the Doppler shifts of different transition region and coronal lines as a function of the line formation temperature for the timestep  $t=30$  min of the simulation. In Fig. 2

we display the corresponding two-dimensional Doppler shift map of the C IV (1548 Å) line for that timestep. The map clearly shows the dominance of redshift in this transition region line which indicates a downflow of material directed towards the solar surface. The coronal mass in the simulation box fluctuates by approximately 0.1% only. Therefore a global sinking of the atmosphere due to mass loss can be ruled out as a mechanism causing the net line shift observed in the C IV line. By tracing magnetic field lines through the simulation box and analyzing flows along the changing magnetic structure of these lines we can investigate the mass cycle between the chromosphere and the corona.

For the tracing of magnetic field lines in the simulation box in time two different techniques are applied. The first one is a field line advection routine included in the VAPOR (Visualization and Analysis Platform for Ocean, Atmosphere, and Solar Researchers) software package (Clyne et al.

2005, 2007). Alternatively, we developed a routine, where it is assumed that the field lines move with the plasma. Both techniques yield similar results for the temporal field line evolution. A field line near a small X-type reconnection site is selected for further analysis. Its temporal evolution is shown in Fig. 3 for some five minutes.

During the course of the simulation the left footpoint of the field line remains roughly in the same place connected to the same photospheric region, whereas the footpoint on the right connects back and forth between two different photospheric regions which is a consequence of the reconnection. In order to investigate the filling and draining of the loop that ultimately leads to the observed Doppler shifts, we extract the vertical velocity at the location of highest C IV intensity along the field line.

A quantitative analysis of the extracted vertical velocities shows a change of sign in velocity as the field line reconnects (see solid line in Fig. 4). In a first phase of the field line evolution (0-8 minutes) a positive velocity, corresponding to an upflow of material, is observed at the location of highest C IV intensity along the loop. After the field line reconnects (from black to dark grey (blue to green) in Fig. 3), the sign of the vertical velocity switches and plasma is now draining out of the loop. Indicated by the dotted lines in Fig. 4 are the spatially fixed regions where the mass loading

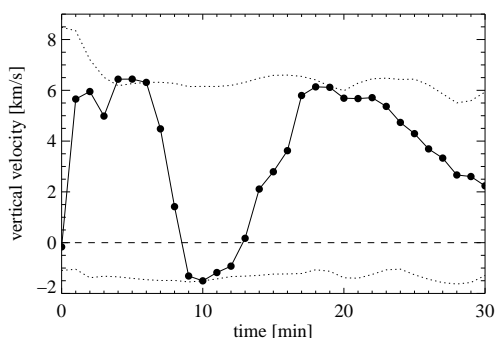


**Fig. 4.** Vertical velocity  $v_z$  at point of highest C IV intensity along the field line as a function of the simulation time.

and draining takes place for a certain timestep. Following the temporal evolution of the velocity at these sites in the simulation box shows that these regions remain stable for the whole simulation run with little variation in their absolute values.

#### 4. Conclusions

In this new scenario of a chromosphere-corona-mass-cycle we suggest that field lines are intermittently connected to sites of increased heating rate where plasma is fed into the loop and to sites with less heating where the plasma undergoes draining. The persistent transition region redshifts are based on the continuously changing three-dimensional magnetic structure, an inherent 3D process, and are not necessarily correctly described by 1D loop models.

#### References

- Bingert, S., Zacharias, P., Peter, H., & Gudiksen, B. 2009, *Advances in Space Research*, in press
- Brandenburg, A., & Dobler, W. 2002, *Comp. Phys. Comm.*, 147, 471
- Clyne, J., Mininni, P., Norton, A., & Rast, M. 2007, *New Journal of Physics*, 9, 301
- Clyne, J., & Rast, M. 2005, *Proceedings of Visualization and Data Analysis*, 284
- Gudiksen, B., & Nordlund, Å. 2002, *ApJ*, 572, L113
- Gudiksen, B., & Nordlund, Å. 2005a, *ApJ*, 618, 1020
- Gudiksen, B., & Nordlund, Å. 2005b, *ApJ*, 618, 1031
- Parker, E. N. 1972, *ApJ*, 174, 499
- Parker, E. N. 1983, *ApJ*, 264, 624
- Peter, H., & Judge, P. G. 1999, *ApJ*, 522, 1148
- Peter, H., Gudiksen, B. V., & Nordlund, Å. 2004, *ApJ*, 617, L85
- Peter, H., Gudiksen, B. V., & Nordlund, Å. 2006, *ApJ*, 638, 1086
- Zacharias, P., Bingert, S., & Peter, H. 2009, *Advances in Space Research*, 43, 1451